COMPOSITIONAL AND THERMOPHYSICAL STRATIGRAPHY IN MARS' MOUND DEPOSITS

Ari H. D. Koeppel[1] (akoeppel@nau.edu), C. S. Edwards[1], A. M. Annex[2], K. W. Lewis[2]. [1]Northern Arizona University, Dept. of Astronomy and Planetary Science; [2]Johns Hopkins University, Dept. of Earth and Planetary Science

Introduction:

Layered sedimentary deposits within equatorial craters on Mars record histories of crater infilling [1]. Orbital detections of hydrated alteration minerals [2] in these Noachian to Hesperian-aged [3,4] deposits suggest that dynamic, volatile-rich and potentially habitable ancient environments may have once existed within these regions [5,6]. Because of the implications for water-rich and habitable environments, infilled craters have been the focus of multiple rover missions [7–9].

While new information from rovers and satellites has yielded significant advances, our understanding of the origins of various styles of crater infill deposits remains poorly constrained. Among the proposed depositional mechanisms for intracrater layered deposits are aeolian airfall dust [1,3], pyroclastic ejecta [10], impact surges [11], fluvio-lacustrine deposition [3], groundwater upwelling [4,12] and seasonal ice deposit layering/melting [13–15]. Each depositional style is expected to produce deposits with distinct chemical and thermophysical properties, however the extensive dust cover in Arabia Terra and many other cratered regions has thus far limited detailed interpretations of spectral imagery.

In this study, we pair advanced spectral data processing and denoising [16,17] with a statistical approach to visualizing orbital datasets in order to uncover how different crater infill types exhibit relationships between mineral signals and thermal inertia. We are interested using these correlations in order to better differentiate between inherent deposit properties and obscuring dust cover, which will allow us to determine the physical properties, and thus the likely depositional styles, of different strata within mounds.

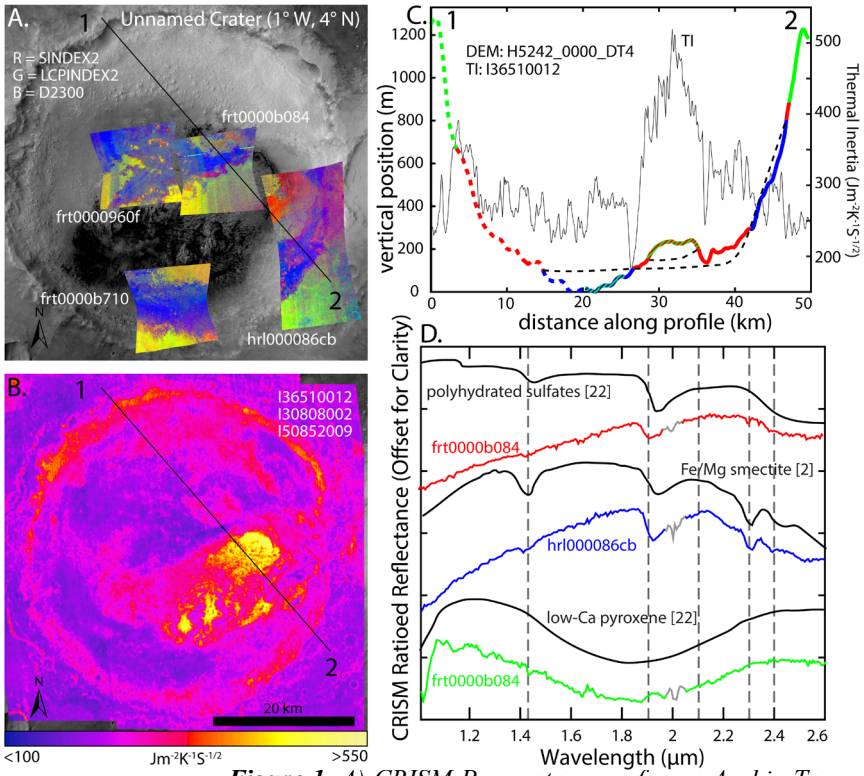

***Figure 1**. A) CRISM Parameter map for an Arabia Terra crater. (R = SINDEX2 G = LCPINDEX2, B = D2300) [22]. B) THEMIS-derived TI map. C) HRSC DEM profile colored to promiant mineralogies with TI along track. D) CRISM ratioed spectra of prominent mineral types with lab references. This crater yielded over 10^6 sample points.*

Methods:

Thermal Inertia: Thermal inertia (TI) is a material property stemming from thermal conductivity, density and heat capacity. For geologic materials, higher TIs are associated with dust-free deposits, compacted surfaces and bedrock. Rocky materials on Mars (e.g. crystalline lavas or lithified sediment) vary from around 500 to >1200 $Jm^{-2}K^{-1}s^{-1/2}$ [18]. We derive pixel-by-pixel TI values for each crater of interest using nighttime Thermal Emission Imaging System (THEMIS, ~100 m/px, TIR) [19] imagery and implementing the KRC simulated one point mode thermal model [16,20]. The model accounts for slope angle, solar azimuth, albedo and previous TI estimates made at lower resolution [21].

Mineralogy: Compact Reconnaissance Imaging Spectrometer for Mars (CRISM, 18 m/px, VNIR) targeted hyperspectral observations were also processed for each region. After applying an atmospheric correction, spectra were acquired by ratioing regions of interest to spectrally bland locations in the same image column. Parameter maps [22] were then produced using a denoising routine outlined in [17].

Data Clustering: Datasets were spatially aligned and resampled to 18 or 36 m/px (full or half CRISM resolution). For each crater, pixel raster values for CRISM band parameters, TI, and lambert albedo were first plotted by kernel density in order to qualitatively

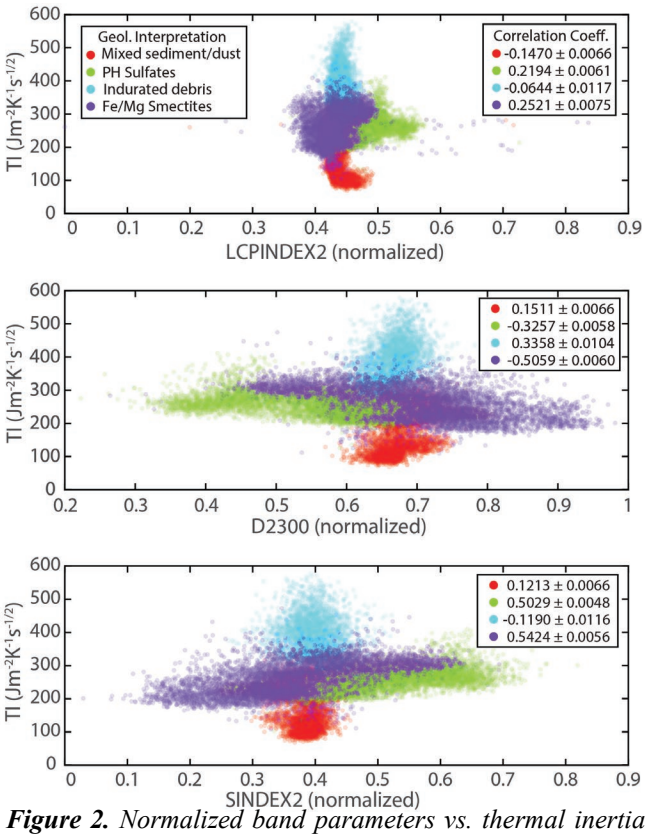

Figure 2. *Normalized band parameters vs. thermal inertia for the four CRISM stamps in Fig 1, clustered (colors) using Gaussian Mixture Modelling of normalized data subsets. The clusters correspond with dominant geologic materials and mixtures within the craters. Correlation coefficients of the specific band parameters vs TI, and their 95% confidence intervals are shown for each cluster.*

identify the number of clusters present. All data was then normalized, and we conducted a principal components analysis. For principal components that explained more than 20% of the normalized sample variance, the key parameters (coefficient > 0.30) were identified. Using only these key parameters and the estimated number of clusters, we then applied a gaussian mixture model to the data to determine a cluster probability for each data point. Correlation coefficients were then calculated between all parameters for each individual cluster.

Results and Discussion:

Data clustering and statistical analysis reveals trends that may be difficult to discern by eye in spectral datasets. The clustering methods used in this study tended to identify the prominent geologic material types within each scene and gave values for their characteristic TI ranges and band parameter strengths. They also revealed relationships between TI and band parameter strength for different material types.

Mars' sedimentary mounds often show a mantling dust cover that conceals mineral signals and lowers observed surface TIs. If mineral detections in cohesive deposits are primarily controlled by dust cover, then there should nearly always be a positive correlation between relevant band parameters and TI. Alternatively, if identifiable band depths are present in the spectral data, but there is not always a positive correlation with TI, this would indicate that the modelled TI values are representative of the rock units themselves and can then be used to infer the material properties of those deposits. The physical properties of sedimentary deposits (such as grain size, degree of induration, cementation and porosity) are key to determining possible depositional styles and alteration histories.

Our initial results suggest that the TIs of some hydrated mineral deposits do represent inherent thermophysical properties rather than signals dictated by dust cover, likely because those surfaces are actively eroding and cannot retain a dust mantle. Observed low crater densities in the mounds support this. Within western Arabia Terra craters, polyhydrated sulfates seem to appear in semi-consolidated deposits that overlie more poorly consolidated phyllosilicate deposits. A possible formation mechanism for this sequence would be an airfall dust process with prior or concurrent alteration by ice or groundwater.

Future Work:

Further constraints will require more detailed models of thermophysical properties following deposition and alteration processes. Future work will also include expansion to study other infilled craters on Mars for a global statistical distribution.

Acknowledgements:

CRISM processing assistance from Y. Itoh for stamps not discussed in this work is appreciated. This work is funded in part by the NASA Mars Data Analysis Program (16-MDAP16_2-0118).

References: [1] Lewis, K. & Aharonson, O. (2014) *JGR E* 119 [2] Wiseman, S. *et al.* (2010) *JGR* 115 [3] Edgett, K. & Malin, M. (2002) *GRL* 29 [4] Pondrelli, M. *et al.* (2015) *Bull. GSA* 127 [5] Kite, E. *et al.* (2016) *JGR E* 121 [6] Cabrol, N. *et al.* (1999) *Icarus* 139 [7] Goudge, T. *et al.* (2017) *EPSL* 458 [8] Cabrol, N. *et al.* (2003) *JGR E* 108 [9] Grotzinger, J.P. *et al.* (2015) *Science* 350 [10] Hynek, B.M. & Phillips, R.J. (2008) *EPSL* 274 [11] Knauth, L.P. *et al.* (2005) *Nature* 438 [12] Andrews-Hanna, J.C. & Lewis, K.W. (2011) *JGR E* 116 [13] Cadieux, S.B. & Kah, L.C. (2015) *Icarus* 248 [14] Niles, P.B. & Michalski, J. (2009) *Nat. Geosci.* 2 [15] Baioni, D. *et al.* (2014) *PSS* 104 [16] Kieffer, H.H. (2013) *JGR E* [17] Pan, L. *et al.* (2017) *JGR E* 122 [18] Edwards, C.S. *et al.* (2009) *JGR E* 114 [19] Christensen, P.R. *et al.* (2004) *SSR* 110 [20] Edwards, C.S. & Piqueux, S. (2016) *GRL* 43 [21] Putzig, N.E. *et al.* (2005) *Icarus* 173 [22] Viviano-Beck, C.E. *et al.* (2014) *JGR* 119